IJE TRANSACTIONS B: Application Vol. 26, No. 8, (August 2013) 845-858

International Journal of Engineering

Journal Homepage: www.ije.ir

Adsorption of Fe(II) from Aqueous Phase by Chitosan: Application of Physical Models and Artificial Neural Network for Prediction of Breakthrough

H. Radnia[a], A. A. Ghoreyshi[a,*], H. Younesi[b], M. Masomi[a], K. Pirzadeh[a]

[a] *Chemical Engineering Department, Babol University of Technology, Babol, Iran*
[b] *Department of Environmental Science, Faculty of Natural Resources, Tarbiat Modares University, Noor, Iran*

PAPER INFO

Paper history:
Received 28 February 2013
Received in revised form 01 April 2013
Accepted 18 April 2013

Keywords:
Chitosan
Fe(II)
Adsorption
Breakthrough Curve
Artificial Neural Network

ABSTRACT

Removal of Fe(II) from aqueous media was investigated using chitosan as an adsorbent in both batch and continuous systems. Batch experiments were carried out at initial concentration range of 10-50 mg/L and temperature range of 20–40˚C. In batch experiments, maximum adsorption capacity of 28.7 mg/g and removal efficiency of 93% were obtained. Adsorption equilibrium data were well-fitted with Langmuir-Freundlich model and the model parameters were obtained. In column study, experiments were performed in a fixed bed of chitosan operated at continuous up-flow mode and constant temperature of 25˚C. Sharp breakthrough curves were observed at high flow rates, high inlet metal concentrations and low bed heights. Breakthrough curves were analyzed by physical models such as Thomas and Yan's models as well as Artificial Neural Network (ANN) method. Compared to physical models, simulation of dynamic behaviour of the system using Back Propagation Artificial Neural Network (BP-ANN) demonstrated high coincidence between experimental and predicted breakthrough curves. The FTIR spectrum of chitosan before and after adsorption process demonstrated that hydroxyl and amino groups are the main functional groups involved in the binding of Fe(II).

doi: *10.5829/idosi.ije.2013.26.08b.06*

NOMENCLATURE

a_i	output value of ith neuron	N	coefficient in Freundlich isotherm model
A	Yan model constant	Q	influent volumetric flow rate (mL/min)
b_i	ith neuron bias	q_e	metal uptake capacity at equilibrium (mg/g)
B	coefficient in Langmuir–Freundlich isotherm model	q_m	maximum metal uptake capacity predicted by isotherms (mg/g)
C_0	initial metal concentration (mg/L)	q_T	maximum metal uptake capacity predicted by Thomas model (mg/g)
C_e	equilibrium metal concentration (mg/L)	q_Y	maximum metal uptake capacity predicted by Yan model (mg/g)
C_t	effluent metal concentration at time t in column (mg/L)	R	removal efficiency (%)
H	bed height (cm)	R^2	determination coefficient
H_m	mass transfer zone (cm)	t	time (min)
k_F	Freundlich equilibrium constant (mg/g (L/mg)$^{1/n}$)	T	solution temperature (°C)
k_L	Langmuir equilibrium constant (L/mg)	t_b	breakthrough time (min)
k_{LF}	Langmuir–Freundlich equilibrium constant (L/mg)	t_e	exhaustion time (min)
k_T	Thomas rate constant (mL/mg.min)	V_0	initial volume in batch system (L)
M	mass of used adsorbent (g)	V_e	final volume in batch system (L)
$m_{adsorbed}$	amount of metal ions adsorbed in the column (mg)	V_{eff}	treated effluent volume in column (mL)
m_{total}	total amount of metal ions sent to the column (mg)	W_{ij}	connection weight from a neuron (i) to the neuron (j)
n_i	net input to neuron i	X_j	input vector of neuron j

* Corresponding Author Email: aa_ghoreyshi@nit.ac.ir (A. A. Ghoreyshi)

1. INTRODUCTION

Wastewater containing large amounts of heavy metals especially iron should be treated before being discharged into environment. Exposure to iron for a long time can cause vomiting, coma, gastrointestinal bleeding, convulsions, and jaundice [1]. It is also reported that the accumulation of iron in the brain causes diseases such as Parkinson, Alzheimer and other genetic disorders [2]. The World Health Organization (WHO) decleres a maximum admissible concentration of iron of 0.3 mg/L in drinking water [3]. Iron can also create undesirable problems in ecosystems or industrial processes in its high concentrations [4].

Several technologies have been developed for removal of iron, such as membrane technologies [5], ion exchange [6], extraction [7], precipitation [8], Electro coagulation [9], adsorption [10, 11], etc. Recently, Fu and Wang [12] have evaluated the latter method in order to treat wastewaters containing heavy metals. As a result, adsorption was recognized as an effective and economic method for heavy metal removal. However, combination of these technologies can be used if certain specifications are required [13].

Adsorption process can be carried out in a batch or continuous systems [14]. The main objective of the adsorption study in batch system is to assess the adsorption capacity of metal ions by the adsorbent for practical applications. It provides useful information about the effectiveness of a specific adsorbent-metal system. Generally, adsorption data obtained in batch systems are not applicable to most treatment systems. Continuous adsorption studies are necessary to evaluate the technical feasibility of the process for large scale applications. Among different column configurations, packed bed columns have been recognized as an effective, economic and the most convenient method for adsorption processes [15]. Design of an adsorption column may require laboratory testing to determine the breakthrough curve.

Choosing a suitable adsorbent plays an important role in the efficiency of adsorption process. Chitosan is an effective natural macromolecule adsorbent [16] which has a great tendency to bind to metal ions due to a large number of hydroxyl and amino groups on its structure [17]. Numerous batch studies were carried out on removal of heavy metals using pure chitosan or its derivatives [18-21]. Wan Ngah et al. [22] have investigated adsorption of heavy metals and dyes by various chitosan composites. In a review paper, the abilities of pristine and modified chitosan for adsorption of selected heavy metals including Cu(II), Zn(II), Ni(II), Cd(II) and Pb(II) from aqueous media have been evaluated by Wu et al. [23].

In contrast to batch studies, only a few research works have been focused on employing chitosan in packed bed column for the removal of heavy metals. Application of immobilized chitosan on bentonite in a continuous flow packed column for the removal of Cu(II) from aqueous solution have been investigated [24]. In addition, Chen et al. [13] studied the removal of arsenic (As) from water by molybdate-impregnated chitosan beads in both batch and continuous operations. Removal of Cr(VI) by xanthated chitosan has been investigated in a packed bed up-flow column [25]. In another investigation, the cross-linked chitosan in a packed-bed column was used to remove Cu(II) from water [26]. Kavianinia et al. [27] prepared a new efficient, low cost chitosan based biosorbent. They employed new sorbent in a fixed bed column for the adsorption of Cu (II) ions from an aqueous solution. Dynamic and static adsorption and desorption of Hg(II) ions using membranes and spherical shapes of chitosan were studied [28].

Researches performed on removal of iron, compared to other heavy metals, in a packed bed column are rare. The potential of commercially prepared wooden charcoal for the removal of mono- and binary-metal ion systems consist of Fe(II) and As(III) was tested in column studies [29]. Also, simultaneous biosorption of Cr(VI) and Fe(III) on free *Rhizopus arrhizus* was investigated in a packed column and the results were compared to the removal of single metal ion [30].

There are few reports dealing with chitosan as an adsorbent for iron removal from water [31]. These investigations have been carried out in batch systems and suffered from a lack of continuous data. Hence, the main objective of the present study was to assess the potential of chitosan for adsorption of iron through batch and continuous experiments. In batch experiments, equilibrium data for isotherm models were obtained. The effect of design parameters, such as flow rate, bed height and inlet metal concentration on column performance and shape of the breakthrough curves was also evaluated in column study. In addition, kinetic column models, namely Thomas and Yan models were applied to describe the dynamic performance of the adsorption process and assisted in prediction of the breakthrough curves. Artificial neural network (ANN) is extensively used for modeling of complex systems where the physical modeling was difficult. In this work, the column dynamic adsorption behavior was also modeled by ANN method and the results were compared to the predicted values by physical models.

2. MATERIALS AND METHODS

2. 1. Chemicals and Materials Chitosan with minimum deacetylation of 85% was purchased from Sigma-Aldrich (USA). All other chemicals used in this study were purchased from Merck (Darmstadt,

Germany). All reagents were analytic grade and used without further purification. Stock solution of 1000 mg/L of Fe(II) ions was prepared using crystallic heptahydrate ferrous sulfate salt. In order to achieve the desired concentration, the stock solution was diluted by adding adequate amount of double distilled water. The pH of the metal solution was adjusted to its optimum value, 4, by adding sufficient amounts of 0.1M HCl and NaOH solutions.

2. 2. Batch Experiments Batch adsorption experiments were carried out by mixing 0.15 g of chitosan with 100 mL of solutions at different initial concentrations of Fe(II) in the range of 10–50 mg/L. The mixture was equilibrated at 180 rpm in incubator shaker (model KS 4000i control, IKA) for 4 h. Samples were taken at fixed time intervals. The adsorbent was separated from the samples using 0.45μm syringe filter. Iron concentrations in the filtrates were analyzed by 5-sulfosalicylic acid (SSA) reagent, using a UV–Vis Spectrophotometer (model 2100 SERIES, UNICO) at λmax = 425 nm [32]. The equilibrium was achieved when no change was observed in the concentration of solution. Experiments were carried out at three different constant temperatures, i.e. 20, 30 and 40 °C.

2. 3. Continious Column Experiments Fixed-bed adsorption studies were carried out in a glass column of 20 cm height and 6 mm internal diameter in an up-flow mode. The column diameter was deliberately chosen small to ensure that the flow pattern in the column is in plug form. A fixed mesh was used at the bottom of column in order to keep adsorbent content inside the column and also to create a uniform flow distribution throughout the column. Sufficient amounts of chitosan were loaded into the column to yield a desired bed height. A layer of glass wool was used at the top of column to avoid the adsorbent loss.

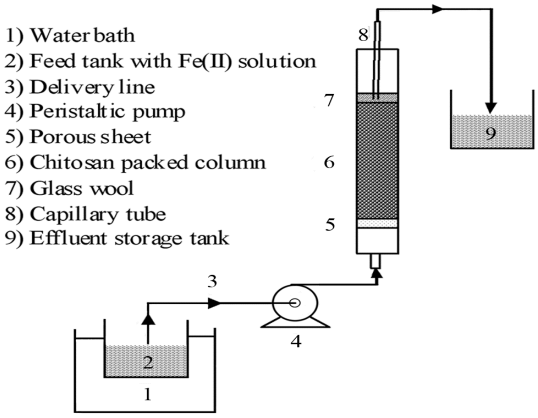

Figure 1. Schematic diagram of the experimental set up for fixed bed studies.

The layer also prevented the adsorbent floating to ensure a closely packed arrangement. A capillary tube was placed in the middle of the glass wool to allow the effluent leave the column rapidly. The feed tank was placed in a water bath to keep feed temperature constant at 25˚C; also the column external walls were thermally isolated to ensure the isothermal adsorption process. The schematic diagram of the column setup is shown in Figure 1.

Fe(II) solution with a known concentration was fed upward through the column at constant flow rates controlled by a peristaltic pump. Samples were collected at regular time intervals from the effluent stream to analyze for residual metal concentration. Samples collection continued till the effluent and influent concentrations were become equal.

3. RESULTS AND DISCUSSION

3. 1. Batch Study The main factors affecting on adsorption capacity such as pH, adsorbent dosage and temperature were investigated in batch study. pH of the solution were studied between 3.5 to 6 and the optimum pH was obtained at 5. Furthermore, the effect of adsorbent dosage was investigated in the range of 1.5-10 g/l and results revealed that 1.5g/ l of the solution was the optimum dosage. Therfore, all further batch experiments to determine adsorption isotherms were carried out at these optimum pH and adsorbent dosage. Moreover, temperature has a considerable effect on adsorption capacity and removal efficiency of Fe(II) by chitosan. The impact of temeperature was studied within temperature range of 20-40°C. Two important parameters in batch adsorption studies are removal efficiency and metal uptake capacity. Both high removal efficiency and metal uptake capacity indicate an effective adsorption process. The removal efficiency (%R) is defined as:

$$\%R = \frac{C_0 - C_e}{C_0} \times 100 \quad (1)$$

where, C_0 and C_e are metal concentrations at the initial and equilibrium conditions (mg/L), respectively.

Experimental data obtained in batch study demonstrated that removal efficiency was in the range of 75 to 93%. The removal efficiency had an inverse relationship with temperature as well as initial concentration. Therefore, maximum removal efficiency was observed at the lowest temperature and initial metal concentration under study.

The amount of metal ion adsorbed by chitosan in batch system was also calculated according to the following equation [33]:

$$q_e = \frac{C_0 V_0 - C_e V_e}{m} \quad (2)$$

where, q_e is the equilibrium concentration of Fe(II) in sorbed phase known as metal uptake capacity (mg/g), V_0 and V_e denote the initial and final volume (L), respectively and m represents the mass of used adsorbent (g). The amount of equilibrium uptake was plotted against the concentration of iron in the solution at equilibrium state to determine adsorption isotherm. Equilibrium adsorption data were correlated with several isotherm models such as Langmuir, Freundlich and Langmuir–Freundlich isotherms. These models are expressed by Equations (3), (4) and (5), respectively [34]:

$$q_e = \frac{q_m k_L C_e}{1 + k_L C_e} \quad (3)$$

$$q_e = k_F C_e^{1/n} \quad (4)$$

$$q_e = \frac{q_m (k_{L.F} C_e)^b}{1 + (k_{L.F} C_e)^b} \quad (5)$$

In the above equations q_e is the amount of metal adsorbed per unit weight of adsorbent at equilibrium (mg/g), C_e is the equilibrium metal concentration in solution (mg/L), q_m is the maximum uptake of adsorbent (mg/g). k_L (L/mg), k_F (mg/g (L/mg)1/n) and $k_{L.F}$ (L/mg) are the Langmuir, Freundlich and Langmuir–Freundlich equilibrium constants, respectively. The exponent coefficients of n and b are dimensionless heterogene coefficients in Freundlich and Langmuir–Freundlich models . The model parameters were recovered through a nonlinear fit of experimental uptake data with model equations. Figure 2 shows the experimental adsorption isotherms of Fe(II) at three different temperatures along with the model predicted values. As it can be seen in Figure 2, all three models fitted the experimental data well. The model parameters as well as regression correlation coefficients (R^2 values) have been listed in Table 1. With respect to regression correlation coefficients, data exhibited the best fit to Langmuir–Freundlich model. As well, the maximum uptake capacity (q_m) predicted by Langmuir–Freundlich model decreased with an increase in temperature which is in accordance with experimental data. The value of parameter n in Freudlich isotherm is an indicator of variation in bond energies with surface density [20]. From Table 1, all n values obtained are greater than 1 and lie in the range 1.36-1.66. Therefore, it can be deduced that in adsorption of ferrous ions by chitosan, bond energies decreased with the surface density.

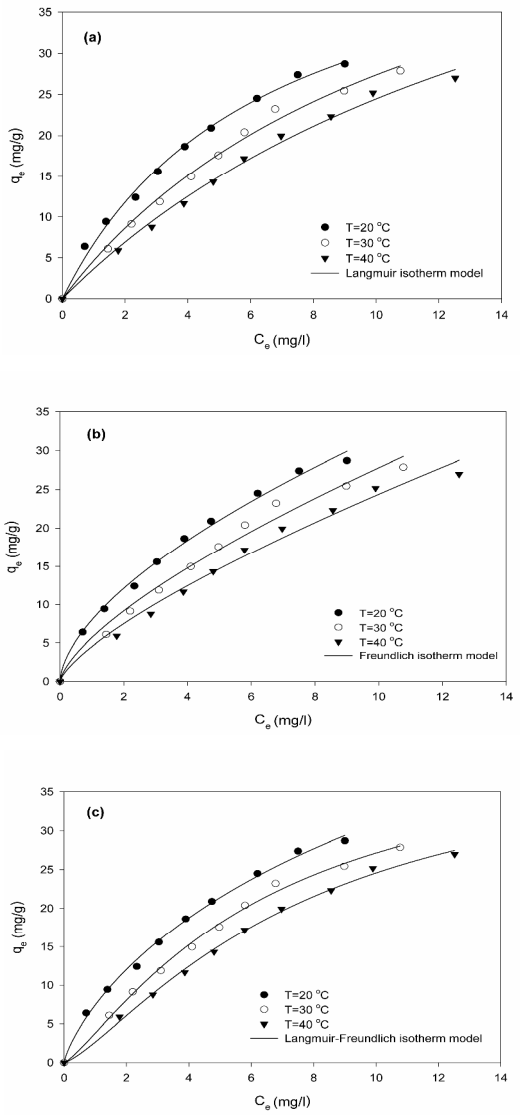

Figure 2. Adsorption isotherms of Fe(II) on chitosan fitted to (a) Langmuir, (b) Freundlich and (c) Langmuir Freundlich isotherm models at three different temperatures.

TABLE 1. Adsorption isotherm constants for Fe(II) ions adsorbed by chitosan

T (°C)	Langmuir			Freundlich				Langmuir-Freundlich			
	k_L	q_m	R^2	R_L	k_F	N	R^2	$k_{L.F}$	q_m	B	R^2
20	0.1574	49.40	0.9953	0.11−0.38	8.0027	1.66	0.9955	0.0554	80.27	0.78	0.9972
30	0.0847	59.69	0.9947	0.19−0.54	5.6955	1.45	0.9862	0.1575	42.49	1.25	0.9967
40	0.058	66.65	0.9948	0.25−0.63	4.5222	1.36	0.9873	0.1311	41.74	1.32	0.9977

TABLE 2. The breakthrough parameters for Fe(II) adsorption onto chitosan at different bed heights, flow rates and influent metal concentrations.

C_0 (mg/L)	Q (mL/min)	H (cm)	t_b (min)	t_e (min)	H_m (cm)	V_{eff} (mL)	q_e (mg/g)	R (%)	C_e (mg/L)
30	2	8	75	660	7.09	1320	48.5	52	13.5
30	4	8	65	420	6.76	1680	51.2	42	16.3
30	6	8	30	210	6.85	1260	34.8	38	17.4
30	4	4	20	210	3.61	840	52.5	41	17.8
30	4	12	95	610	10.13	2440	59.6	49	15.1
10	4	8	150	480	5.50	1920	26.4	56	4.2
50	4	8	16	300	7.57	1200	50.5	34	32.1

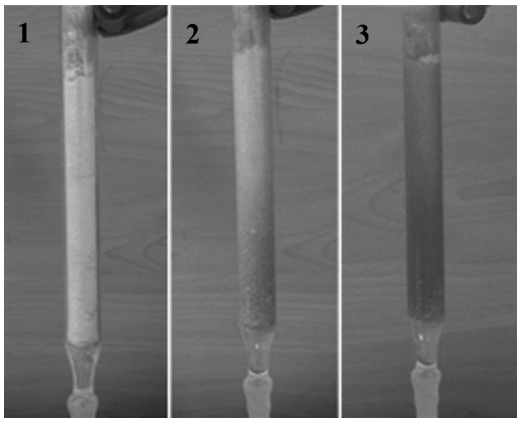

Figure 3. Column during adsorption process.

3. 2. Continious Column Studies Figure 3 shows the column status during adsorption process. It is obvious that at the first status (1), the adsorbent was fresh with all its adsorption sites. At the beginning of the adsorption process, most of the irons were adsorbed on chitosan due to the existence of a plenty of vacant pores. As time passed, some of the adsorption sites were occupied and metal concentration in the effluent started gradually to rise (2). When all available sites on the adsorbent were occupied, the inlet and outlet concentrations became identical (3).

The breakthrough curve was obtained by plotting the metal concentration (normalized concentration) at the column exit as a function of time for a given bed height [35]. The effects of flow rate (2, 4 and 6 mL/min), chitosan bed height (4, 8 and 12 cm) and inlet metal concentration (10, 30 and 50 mg/L) on the breakthrough characteristics of the adsorption process were investigated. Results have been shown in Figures 4-6. For all curves, when the adsorption was continued beyond the breakthrough point, the C_t/C_0 rapidly rose to the value about 0.5 and then approached slowly to the value of 1.

The breakthrough curves need to be examined quantitatively. The breakthrough time, t_b (min), is the time at which metal concentration in the effluent reaches 5% of the influent concentration (C_t/C_0=0.05). The bed exhaustion time, t_e (min), is the time at which the metal ions concentration in the effluent exceeds 90% of the concentration in the influent (C_t/C_0=0.9). The two significant parameters were used to evaluate the mass transfer zone, H_m (cm), given by Equation (6):

$$H_m = H \times (\frac{t_e - t_b}{t_e}) \quad (6)$$

where, H is the total length of the sorption bed (cm). The treated effluent volume, V_{eff} (mL), can be calculated from Equation (7),

$$V_{eff} = Q \times t_e \quad (7)$$

where, Q is the influent volumetric flow rate (mL/min). The total amount of metal ions sent to the column, m_{total} (mg), is given by the following equation:

$$m_{total} = \frac{Q C_0 t_e}{1000} \quad (8)$$

The total mass of metal adsorbed in the column, $m_{adsorbed}$ (mg), is represented by the area above the breakthrough curve, which is expressed by Equation (9):

$$m_{adsorbed} = \frac{Q C_0}{1000} \int_0^{t_e} (1 - \frac{C_t}{C_0}) dt \quad (9)$$

In this work, a computer program MATLAB 7. 2 (R2008a) was used to obtain this area through numerical integration. The equilibrium adsorption capacity of the column, q_e (mg/g), can be determined from the ratio of amount of adsorbed metal, $m_{adsorbed}$ (mg), and the amount of the chitosan loaded in the column, m (g).

$$q_e = \frac{m_{adsorbed}}{m} \quad (10)$$

This refers to a point on the equilibrium isotherm corresponding to the final equilibrium concentration (C_e) in the column. The equilibrium metal concentration, C_e (mg/L), is determined from the following equation:

$$C_e = \frac{m_{total} - m_{adsorbed}}{V_{eff}} \times 1000 \quad (11)$$

Finally total metal removal (%) can be calculated from the ratio of adsorbed metal mass, $m_{adsorbed}$ (mg), to the total amount of metal ions sent to the column , m_{total} (mg), as follows,

$$\%R = \frac{m_{adsorbed}}{m_{total}} \times 100 \quad (12)$$

The calculated parameters for different operating conditions are summarized in Table 2. For a good adsorption process a delayed breakthrough, earlier exhaustion, steep breakthrough curve, shortened mass transfer zone, high uptake and high removal efficiency would be expected [15].

3. 2. 1. Effect of Flow Rate The influence of flow rate on the shape of breakthrough curve is illustrated in Figure 4. At higher flow rates, the slope of breakthrough curve increased and exhaustion time occurred in a shorter time. According to Table 2, an increase in flow rate from 2 to 6 mL/min, caused a drastic decrease in exhaustion time. This can be explained by knowing that with an increase in flow rate, additional amount of metal in the solution was contacted with the adsorbent. An increase in flow rate caused an enhancement in mass transfer rate and therefore led to rapid chitosan saturation. Subsequently, more amounts of metal ions will be adsorbed in a fixed bed height. This is also true for an increase in flow rate from 2 to 4 mL/min. In this case, the increase in adsorption capacity from 48 to 51 mg/g was observed.

On the other hand, increase in flow rate decreased retention time of the solution in the column and consequently there was not enough time for metal ions to diffuse through the adsorbent particles. In other words, the faster movement of iron ions through the packed will shorten the residence time of the pollutant in the column. Indeed, liquid leaves the column before equilibrium is achieved. Therefore, it would be highly probable that the inlet metal solution leaves the bed without considerable changes in its concentration while the adsorbent is not saturated yet. In this situation, it may be wrongly supposed that the column has reached to exhaustion time. The intense decrease in metal uptake capacity to 34 mg/g in flow rate of 6 mL/min may be due to this fact.

With an increase in flow rate from 2 to 6 mL/min, removal efficiency decreased from 52 to 38%. Similar observations was reported by the other researchers [24]. This observation may be attributed to disturbance of the film surrounded the adsorbent particle at high flow rate which led reduction in adsorption of metal ions on the chitosan surface. As a result, the ratio of adsorbed Fe (II) ions to the total amount of ions entered in the column, reduced and consequently removal percentage decreased. The calculated equilibrium concentration increased which indicates lower efficiencies of adsorption process at higher flow rates.

In this work, the flow rate of 4 mL/min with the maximum uptake capacity of 51.22 mg/g was the optimum flow rate and was used in further experiments.

Under all examined flow rates, mass transfer zone was almost constant, which is probably due to the same reason that both the t_e and t_b decreased with increasing flow rate. Some previous works confirmed the higher performance of adsorption columns at the lower flow rates [25, 36, 37].

3. 2. 2. Effect of Bed Height As Figure 5 shows, the slope of breakthrough curve decreased at high bed heights due to more amounts of adsorbent loading in the column. This caused an increase in available surface area as well as number of binding sites in adsorbent for metal ions. Therefore, at high bed heights, mass transfer zone needed more time to reach to the end of the column which leads to increase in breakthrough and exhaustion times. As Table 2 shows, the increase in bed height from 4 to 8 cm had not significant effect on removal efficiency and metal uptake capacity, while by increasing the height column to 12 cm considerable changes were observed. The equilibrium concentration of metal ions also decreased at higher bed heights.

As mentioned in some previous works, the metal uptake capacity per unit mass of adsorbent (q_e) is expected to be almost constant for all bed heights [36]. This indicates that the amount of adsorbed metal ions as well as the mass of loaded adsorbent in the column will be increased with using a higher bed height.

Therefore, the metal uptake capacity per unit mass of adsorbent will remain almost constant. In this study, by increasing the bed height to 12 cm metal uptake capacity increased. This could be probably due to increase in retention time which caused the adsorption of metal into inner layers of the adsorbent. It can be concluded that metal uptake capacity is not directly proportional to the amount of adsorbent and also depends on the operating conditions of the column. The similar results have been reported by shahbazi et al. [14].

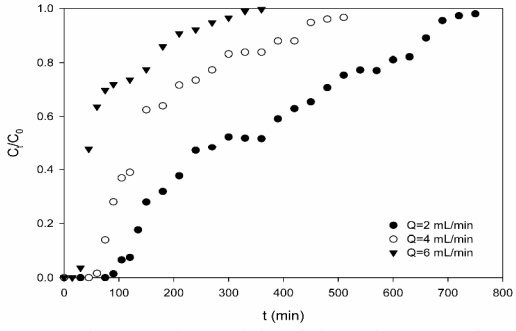

Figure 4. The experimental breakthrough curves for Fe(II) adsorption onto chitosan at different flow rates (H=8 cm; C_0=30 mg/L).

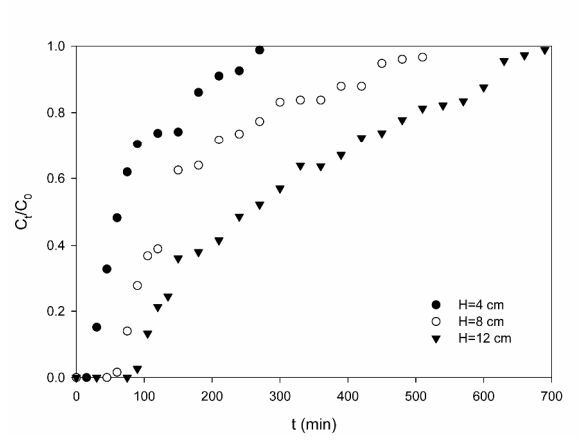

Figure 5. The experimental breakthrough curves for Fe(II) adsorption onto chitosan at different bed heights (Q=4 mL/min; C_0=30 mg/L).

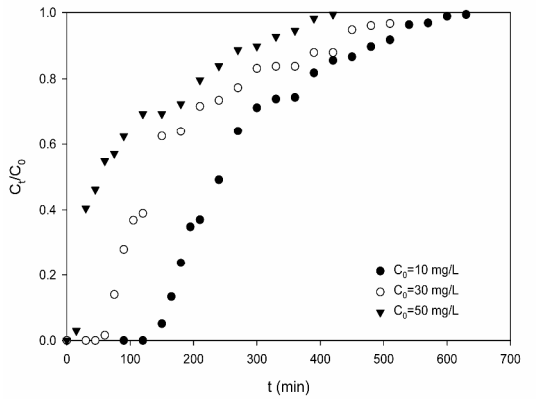

Figure 6. The experimental breakthrough curves for Fe(II) adsorption onto chitosan at different inlet metal concentrations (Q=4 mL/min; H=8cm).

In general, with a higher bed height, larger volumes of the metal solution could be treated compared to a shorter bed; which results in a broadened mass transfer zone. Therefore, based on the needs, the proper bed depth should be designed for a specific application. The effect of bed height on adsorption process was previously investigated by some researchers with similar results [37-39].

3. 2. 3. Effect of Inlet Metal Concentration As it could be observed from Figure 6, breakthrough and exhaustion was occurred in a shorter time and breakthrough curves were much sharper at high inlet concentrations. This is a reasonable behavior because at high inlet concentrations more amounts of metal ions were brought to contact with the adsorbent in the column. Therefore, it became saturated in a shorter time. With respect to values reported in Table 2, change in the inlet concentration affects the column performance. An increase in inlet concentration caused a decrease in the volume of treated effluent and mass transfer zone. At high inlet metal concentrations, additional amounts of metal ions entered the column; but a small portion of them was adsorbed. So, the removal efficiency decreased from 56.3% at the inlet concentration of 10 mg/L to 34.4% at the concentration of 50 mg/L.

On the other hand, the corresponding bed adsorption capacity appeared to increase at higher inlet concentrations. The driving force for adsorption is the concentration gradient between the solute on the surface of the adsorbent and the solute in the bulk phase. Increasing metal concentration in the solution provided higher driving force for adsorption. This resulted in Fe (II) ions adsorption into inner layers of chitosan particles and increased the metal uptake capacity.

These results demonstrated the concentration dependence of the diffusion process. The results are confirmed by a number of previous published articles [24, 36, 40].

3. 2. 4. Fixed Bed Column Modelling In this study, the experimental data obtained for breakthrough time was modeled by two different approaches; i.e. physical models and Artificial Neural Network method.

A. Physical Modeling Modeling of data available from column studies facilitates scale-up potential [41]. In principal, the breakthrough curve is obtained by solving (often numerically) complex partial differential equations which describe material balance and mass transfer equations for bulk and adsorbed phases. However, physical models obtained under simplified conditions are widely used to avoid complexity [42]. To describe the column breakthrough curves obtained at different conditions, Thomas and Yan (modified dose–response) models were used . Thomas model is the most commonly used model in describing of the column performance of breakthrough curves [24]. It is given by the equation below:

$$\frac{C_t}{C_0} = \frac{1}{1 + \exp(a - bt)} \tag{13}$$

where, $a = k_T q_T m/Q$ and $b = k_T C_0$.

In the above equations, C_0 and C_t are the influent and effluent metal concentration, m is the mass of adsorbent (g), Q is the flow rate (mL/min), t is adsorption time (min), k_T is the Thomas rate constant (mL/mg.min) and q_T is the maximum solid phase concentration of the solute predicted by Thomas model (mg/g). In the recent decade, Yan et al. [43] suggested the modified dose–response (Yan) model. This model minimizes the error resulting from the Thomas model, especially at low or high time periods. It is represented by the following equation:

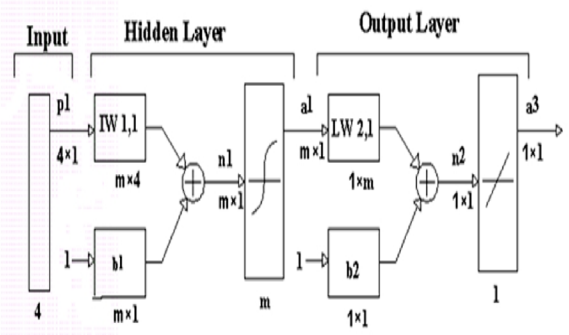

Figure 7. The topological structure of a typical ML-ANN

$$\frac{C_t}{C_0} = 1 - \frac{1}{1 + (\frac{t}{b})^a} \quad (14)$$

where, $b = q_Y m / C_0 Q$ and the constant a are the Yan model constants. It is necessary to state that q_Y is the maximum sorbed phase concentration of the solute predicted by Yan model (mg/g).

B. Artificial Neural Network (ANN) Modeling

Artificial neural networks (ANN) is extensively employed to approximate complex phenomena that is difficult to describe its behavior by conventional modeling techniques, such as mathematical or physical modeling [44]. There are several studies in the literature dealing with ANN applications to predict the behavior of a given system, design new processes and analyze existing processes [45, 46]. The application of ANN for approximation of breakthrough curve in adsorption of heavy metal from water has been investigated [47-49].

ANNs mainly consist of three layers; input, hidden and output layers (see Figure 7). Each input value is represented by a neuron in the input layer. Input values are weighted individually before entering the hidden layer and weighted values are transferred to the hidden layer. The output of the neural network is given by the output layer for the given input data. The main unit of any ANN is an artificial neuron, which has two parts, one is the summing part and the other is multiplied with a weight coefficient and all weighted inputs are summed up. The ith neuron has a summer that collects its weighted input $W_{ij} \bullet X_j$ and the bias b_i to produce its net input n_i, which is expressed by the following equation:

$$n_i = \sum W_{ij}.X_j + b_i \quad (15)$$

where, W_{ij} is the connection weight from a neuron (i) to the neuron (j) that denotes the strength of the connection from the jth input to the ith neuron, X_j is the input vector, b_i is the ith neuron bias [44, 49].

The sum of the weighted inputs is further transformed with a transfer function to get the output value (a_i), according to the following elementary formula [50]:

$$a_i = f(n_i) = f(\sum_{j=1}^{n} W_{ij}.X_j + b_i) \quad (16)$$

There are several transfer functions; the most common is the sigmoidal function [48, 51, 52]. In this study hyperbolic tangent transfer function was used in the hidden layer that calculates output from neuron between −1 and +1, while the linear activation function was employed in the output layer in the model. To find suitable connection weights and biases for each neuron, a training process is essential to set up an ANN as the first step. Several methods can be used for training step. The most utilized one is multilayered neural network called as back propagation (BP) [53]. Before starting the training of ANN, weights are initially randomized. In this study, the Levenberg–Marquardt training algorithm was used for the ANN modeling. The input and output variables in the present study had different characteristics and level resulting into varied response to the neural network. The ANN model training would be more efficient if preprocessing steps are performed on the input and target data for real applications, so that preprocessed data lie between minimum -1 and maximum 1. In order to measure the pollutant removal efficiency and performance of ANN model developed for adsorption process, different types of statistical parameters can be used to estimate the generalized error. In the present work, root of mean squared error value (RMSE) and Pearson's determination coefficient (R^2) were selected to measure the network performance. Statistically, low value of the RMSE satisfies the validation of prediction [53, 54].

In this work, it was preferred to use Multi-layer feed forward Neural Network Architecture (ML-ANN) because of its powerful nonlinear mapping capability [55]. Figure 7 depicts the architecture of the used ANN. The input variables to the neural network were as follows: the treatment time, inlet Fe(II) concentration, flow rate, bed height. The ratio oulet/inlet Fe(II) concentration was chosen as the Neural Network output variable. The number of experimental data used in the ANN was 184 which were divided into two parts: the training set (138 data) and the test set (46 data). The test set was not used in training at all, and it was designed to give an independent assessment of the ANN performance when the design procedure of an overall network was completed. The optimal network was found to have four neurons in input layer, one hidden layer with thirty neurons and one neuron in output layer. The optimal ANN architecture (4:30:1) are shown in Figure 7.

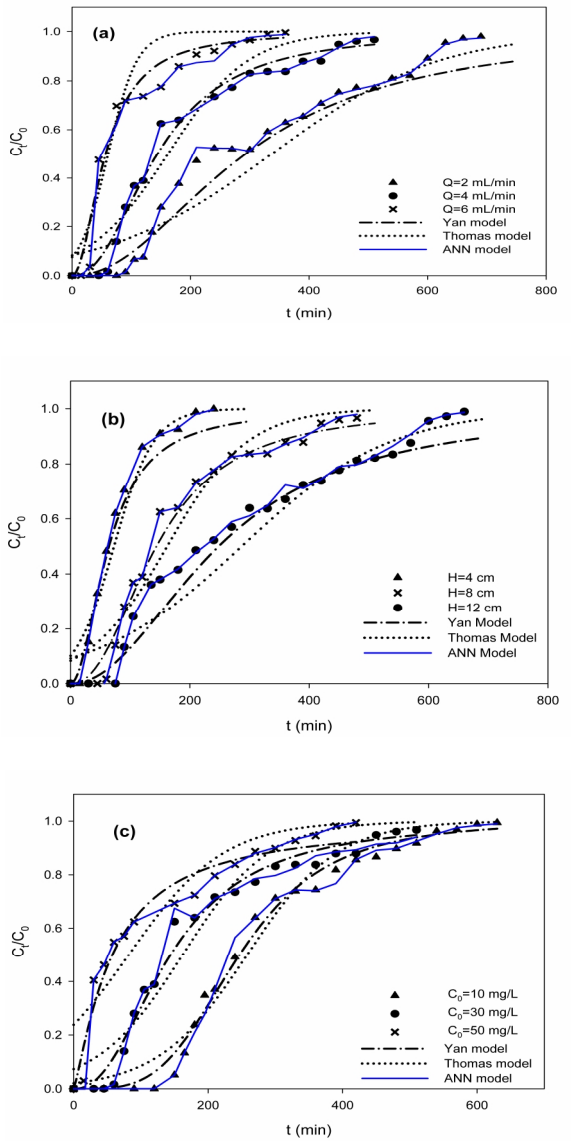

Figure 8. The predicted breakthrough curves by Thomas, Yan and ANN model for Fe(II) adsorption onto chitosan at different (a) flow rates, (b) bed heights and (c) inlet metal concentrations

3. 2. 5. Modelling Results The Thomas and Yan models constants, determined under different conditions, along with the determination coefficients, were presented in Table 3. This was further validated by Figure 8 (a, b and c) in which the predicted breakthrough curves and experimental points were shown at different flow rates, bed heights and influent concentrations, respectively. ANN model results were also shown for comparison in this figure. The recovered parameters of Thomas and Yan's physical models and determination coefficient for all three models have been included in Table 3. It is obvious from Table 3 that the values of Thomas rate constant (k_T), which characterizes the rate of solute transfer from the liquid to the sorbed phase, decreased with increasing initial concentration and bed height. The opposite trend was observed for the column data obtained at various flow rates due to the decrease in the mass transport resistance at high flow rates. The determination coefficient values obtained for Yan model (ranged from 0.9562 to 0.9902), revealed a better agreement with the experimental data compared to the Thomas model (ranging from 0.8686 to 0.9717).

It is clear from Figure 8 that at initial period of adsorption, the Thomas model is not in good agreement with the experimental data. This model has a fixed value when the experimental time is approached to zero (Equation (13); which is in contrast to real conditions. Yan model has covered this limitation at the initial times of column performance. Another important parameter is the prediction of maximum metal uptake capacity by the models. The maximum metal uptake capacity (q) predicted by the Yan model exhibited the same trend predicted by the Thomas model. The predicted values do not coincide exactly with the experimental uptake values but the predicted values of Thomas model is closer to that was experimentally obtained. Therefore, each model has its own advantages in description of experimental data at initial times. Although, Yan's model is an appropriate model from the view point of fitting results, but the better prediction of metal uptake capacity of Thomas's model should not be ignored.

TABLE 3. Parameters predicted from Thomas and Yan model and ANN model for Fe(II) adsorption by chitosan at different bed heights, flow rates and influent metal concentrations.

C_0 (mg/L)	Q (mL/min)	H (cm)	$q_{e\,exp}$ (mg/g)	Thomas model			Yan model			ANN model
				$k_T \times 10^4$ (mL/mg. min)	q_T (mg/g)	R^2	A	q_Y (mg/g)	R^2	R^2
30	2	8	48.57	2.51	47.66	0.9482	2.11	41.41	0.9710	0.9900
30	4	8	51.22	5.22	46.04	0.9317	2.28	41.05	0.9824	0.9965
30	6	8	34.80	14.42	26.05	0.8879	1.98	24.29	0.9562	0.9798
30	4	4	52.56	9.88	44.28	0.9308	1.98	39.10	0.9849	0.9916
30	4	12	59.60	2.68	57.01	0.9521	2.09	49.36	0.9778	0.9974
10	4	8	26.48	15.30	25.34	0.9717	3.76	24.18	0.9902	0.9953
50	4	8	50.55	2.89	40.15	0.8686	1.24	28.30	0.9630	0.9780

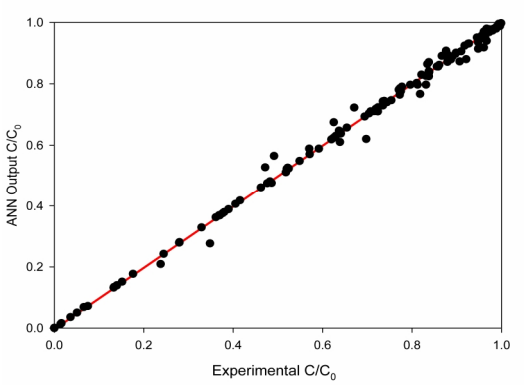

Figure 9. The relationship between experimental data and BP-ANN model outputs

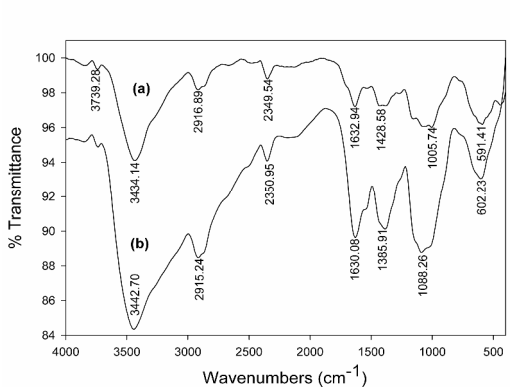

Figure 10. FTIR spectra of chitosan (a) before and (b) after adsorption of Fe(II)

On the other hand, as can be observed from Figure 8 the trained BP-ANN predicted the breakthrough curves almost perfectly compared to physical models. The experimental data and ANN predicted values exactly overlap each other. Figure 9 shows the relationship between experimental data and BP-ANN model outputs. It can be understood that there is the best agreement between calculated and experimental data, which proves that BP-ANN is a most powerful fitting and predictive tool which can describe the column dynamic behavior.

3. 3. FTIR Spectrum of Chitosan The Fourier transform infrared (FTIR) analysis was carried out to identify the functional groups on the chitosan surface that might be involved in the adsorption process. FTIR study is important in order to have valuable information about the mechanism of metal adsorption on chitosan. FTIR spectra of sorbents were recorded by a Shimadzu 8201PC FTIR Spectrometer. 1 mg of the powder was blended with 100 mg of IR-grade KBr and pressed into a tablet. The spectra of the tablets were scanned within the spectral range of 400–4000 cm^{-1}.

The FTIR spectra of the chitosan before and after the adsorption of iron ions have been shown in Figure 10. The spectra display a number of absorption peaks. The broad and strong band ranging from 3200 to 3600 cm^{-1} indicated the presence of OH and NH groups (3434 cm^{-1}). The peaks observed at 2916 cm^{-1} can be assigned to –CH stretching vibration. The peak located at 1632 cm^{-1} is a characteristic of –C=O group due to partial deacetylation of chitosan and it also shows –NH bending vibration bound. The peak at 1428 cm^{-1} corresponds to the –CH bending vibration at $–CH_3$ group. The absorption band at 1005 cm^{-1} represents the stretching C– N [56].

It is known that during the formation of complex species the functional groups absorption can be displaced either below or above the original region of absorption [2]. In this study, the FTIR spectrum for the adsorbent loaded with iron has shown intensity of the peaks were shifted slightly or substantially lower than those in the untouched sample. In addition some shifts in the position of bands suggest the participation of these functional groups in the binding of iron with chitosan.

The frequency numbers of OH and NH groups shifted from 3434 cm^{-1} to 3442 cm^{-1} after iron uptake. Moreover, the sharp shift in the position of the bands from 1428 cm^{-1} and 1005 cm^{-1} to 1358 cm^{-1} and 1088 cm^{-1} was respectively observed. Such shifts show the role of nitrogen in chitosan chemical structure in chemisorption of Fe(II) through formation of complex. This suggests that the mechanism of iron adsorption on chitosan could be due to surface complexation. Similar results have been reported by some previous investigators [19, 21, 57].

4. CONCLUSION

High removal efficiency (92.9%) and metal uptake capacity (28.7 mg/g or 0.514 mmol/g) in batch system demonstrated that chitosan can be used as an effective adsorbent for removal of Fe(II). Based on determination coefficients, a better fit was obtained by examination of the Langmuir-Freundlich isotherm model compared to the Langmuir and Freundlich models.

Removal of Fe(II) in a packed bed system using chitosan has shown an effective and feasible method. A longer breakthrough and exhaustion time occurred at a high bed height, a lower flow rate, and lower influent concentration. Fe(II) uptake capacity of the chitosan bed was strongly dependent on the operational conditions. Maximum uptake capacity (59.6 mg/g or 1.067 mmol/g) was obtained at flow rate of 4 mL/min, bed height of 12 cm and initial concentration of 30 mg/L. With increasing flow rate and inlet metal concentration the

removal efficiency of Fe(II) decreased, while an increase in bed height enhanced the removal efficiency. Maximum removal efficiency in column (56.3%) was obtained at flow rate of 4 mL/min, bed height of 8 cm and inlet Fe(II) concentration of 10 mg/L. Results obtained in the column study indicated that bed adsorption capacities are higher compared to those achieved in batch system due to sufficient concentration gradient during adsorption process in column. But in the best state, the value of removal efficiency was a half of batch system due to low retention time of metal solution in the column. The prediction of breakthrough curves were carried out using the Thomas and Yan models as well as ANN method. The Yan's model provided a good correlation in the prediction of the breakthrough curves in terms of R^2 values. A good agreement was also observed between the simulated breakthrough curves and the experimental data especially at the initial period of column operation using the Yan model. However, the metal uptake capacity values predicted by Thomas model at different conditions were in good agreement with the experimental values. It was observed that Thomas rate constant increased with an increase in flow rate while it decreased with an increase in bed height and inlet metal concentration. On the other hand, applying the BP-ANN approach to predict the column dynamic has gained the best results in terms of maximum match between the experimental and predicted performance. This indicated that the ANN approach can act as a suitable method where it is difficult to describe the system by physical models. The FTIR spectrum for iron loaded adsorbent showed some shifts in the position of bands. It suggests the participation of functional groups, namely hydroxyl and amino groups, in the binding of iron by chitosan.

5. REFERENCES

1. Mohan, D. and Chander, S., "Single, binary, and multicomponent sorption of iron and manganese on lignite". ***Journal of Colloid and Interface Science***, Vol. 299, (2006), 76-87.
2. Hernández, R.B., Franco, A.P., Yola, O.R., López-Delgado, A., Felcman, J., Recio, M.A.L., et al., "Coordination study of chitosan and Fe3+". ***Journal of Molecular Structure***, Vol. 877, (2008), 89-99.
3. WHO, "Guidelines for Drinking-Water Quality", 2 ed, World Health Organizationx, Geneva, Vol. 2, (1996).
4. Kim, D., "Adsorption characteristics of Fe (III) and Fe (III)-NTA complex on granular activated carbon". ***Journal of Hazardous Materials***, Vol. 106, (2004), 67-84.
5. Bernat, X., Pihlajamaki, A., Fortuny, A., Bengoa, C., Stüber, F., Fabregat, A., et al., "Non-enhanced ultrafiltration of iron(III) with commercial ceramic membranes". ***Journal of Membrane Science***, Vol. 334, (2009), 129-137.
6. Lasanta, C., Caro, I., and Pérez, L., "Theoretical model for ion exchange of iron (III) in chelating resins: Application to metal ion removal from wine". ***Chemical Engineering Science***, Vol. 60, (2005), 3477-3486.
7. Li, M., He, Z., and Zhou, L., "Removal of iron from industrial grade aluminum sulfate by primary amine extraction system". ***Hydrometallurgy***, Vol. 106, (2011), 170-174.
8. Nurmi, P., Ozkaya, B., Sasaki, K., Kaksonen, A.H., Riekkola-Vanhanen, M., Tuovinen, O.H., et al., "Biooxidation and precipitation for iron and sulfate removal from heap bioleaching effluent streams". ***Hydrometallurgy***, Vol. 101, (2011), 7-14.
9. Vasudevan, S., Lakshmi, J., and Sozhan, G., "Studies on the Removal of Iron from Drinking Water by Electrocoagulation–A Clean Process". ***Clean–Soil, Air, Water***, Vol. 37, (2009), 45-51.
10. Tahir, S. and Rauf, N., "Removal of Fe (II) from the wastewater of a galvanized pipe manufacturing industry by adsorption onto bentonite clay". ***Journal of Environmental Management***, Vol. 73, (2004), 285-292.
11. Ahamad, K. and Jawed, M., "Kinetics, equilibrium and breakthrough studies for Fe (II) removal by wooden charcoal: A low-cost adsorbent". ***Desalination***, Vol. 251, (2010), 137-145.
12. Fu, F. and Wang, Q., "Removal of heavy metal ions from wastewaters: A review". ***Journal of Environmental Management***, Vol. 92, (2011), 407-418.
13. Chen, C.Y., Chang, T.H., Kuo, J.T., Chen, Y.F., and Chung, Y.C., "Characteristics of molybdate-impregnated chitosan beads (MICB) in terms of arsenic removal from water and the application of a MICB-packed column to remove arsenic from wastewater". ***Bioresource Technology***, Vol. 99, (2008), 7487-7494.
14. Shahbazi, A., Younesi, H., and Badiei, A., "Functionalized SBA-15 mesoporous silica by melamine-based dendrimer amines for adsorptive characteristics of Pb(II); Cu(II) and Cd(II) heavy metal ions in batch and fixed bed column". ***Chemical Engineering Journal***, Vol. 168, (2011), 505-518.
15. Vijayaraghavan, K. and Yun, Y.S., "Bacterial biosorbents and biosorption". ***Biotechnology Advances***, Vol. 26, (2008), 266-291.
16. Varma, A.J., Deshpande, S.V., and Kennedy, J.F., "Metal complexation by chitosan and its derivatives: a review". ***Carbohydrate Polymers***, Vol. 55, (2004), 77-93.
17. Babel, S. and Kurniawan, T.A., "Low-cost adsorbents for heavy metals uptake from contaminated water: a review". ***Journal of Hazardous Materials***, Vol. 97, (2003), 219-243.
18. Paulino, A.T., Guilherme, M.R., Reis, A.V., Tambourgi, E.B., Nozaki, J., and Muniz, E.C., "Capacity of adsorption of Pb2+ and Ni2+ from aqueous solutions by chitosan produced from silkworm chrysalides in different degrees of deacetylation". ***Journal of Hazardous Materials***, Vol. 147, (2007), 139-147.
19. Kyzas, G.Z., Kostoglou, M., and Lazaridis, N.K., "Copper and chromium (VI) removal by chitosan derivatives--Equilibrium and kinetic studies". ***Chemical Engineering Journal***, Vol. 152, (2009), 440-448.
20. Dinu, M.V. and Dragan, E.S., "Evaluation of Cu2+, Co2+ and Ni2+ ions removal from aqueous solution using a novel chitosan/clinoptilolite composite: Kinetics and isotherms". ***Chemical Engineering Journal***, Vol. 160, (2010), 157-163.
21. Vijaya, Y., Popuri, S., Boddu, V., and Krishnaiah, A., "Modified chitosan and calcium alginate biopolymer sorbents for removal of nickel (II) through adsorption". ***Carbohydrate Polymers***, Vol. 72, (2008), 261-271.
22. Wan Ngah, W.S., Teong, L.C., and Hanafiah, M.A.K.M., "Adsorption of dyes and heavy metal ions by chitosan composites: A review". ***Carbohydrate Polymers***, Vol. 83, (2011), 1446-1456.
23. Wu, F.C., Tseng, R.L., and Juang, R.S., "A review and experimental verification of using chitosan and its derivatives as adsorbents for selected heavy metals". ***Journal of Environmental Management***, Vol. 91, (2010), 798-806.

24. Futalan, C.M., Kan, C.C., Dalida, M.L., Pascua, C., and Wan, M.W., "Fixed-bed column studies on the removal of copper using chitosan immobilized on bentonite". ***Carbohydrate Polymers***, Vol. 83, (2011), 697-704.
25. Chauhan, D. and Sankararamakrishnan, N., "Modeling and evaluation on removal of hexavalent chromium from aqueous systems using fixed bed column". ***Journal of Hazardous Materials***, Vol. 185, (2011), 55-62.
26. Osifo, P.O., Neomagus, H.W.J.P., Everson, R.C., and Webster, A., "The adsorption of copper in a packed-bed of chitosan beads: Modeling, multiple adsorption and regeneration". ***Journal of Hazardous Materials***, Vol. 167, (2009), 1242-1245.
27. Kavianinia, I., Plieger, P.G., Kandile, N.G., and Harding, D.R.K., "Fixed-bed column studies on a modified chitosan hydrogel for detoxification of aqueous solutions from copper (II)". ***Carbohydrate Polymers***, Vol. 90, (2012), 875-886.
28. Vieira, R.S. and Beppu, M.M., "Dynamic and static adsorption and desorption of Hg(II) ions on chitosan membranes and spheres". ***Water Research***, Vol. 40, (2006), 1726-1734.
29. Ahamad, K.U. and Jawed, M., "Breakthrough studies with mono- and binary-metal ion systems comprising of Fe(II) and As(III) using community prepared wooden charcoal packed columns". ***Desalination***, Vol. 285, (2012), 345-351.
30. Sag, Y., Atacoglu, I., and Kutsal, T., "Equilibrium parameters for the single- and multicomponent biosorption of Cr(VI) and Fe(III) ions on R. arrhizus in a packed column". ***Hydrometallurgy***, Vol. 55, (2000), 165-179.
31. Ngah, W., Ab Ghani, S., and Kamari, A., "Adsorption behaviour of Fe (II) and Fe (III) ions in aqueous solution on chitosan and cross-linked chitosan beads". ***Bioresource Technology***, Vol. 96, (2005), 443-450.
32. Karamanev, D., Nikolov, L., and Mamatarkova, V., "Rapid simultaneous quantitative determination of ferric and ferrous ions in drainage waters and similar solutions". ***Minerals Engineering***, Vol. 15, (2002), 341-346
33. Jeon, C. and Ha Park, K., "Adsorption and desorption characteristics of mercury (II) ions using aminated chitosan bead". ***Water research***, Vol. 39, (2005), 3938-3944.
34. Limousin, G., Gaudet, J.P., Charlet, L., Szenknect, S., Barthes, V., and Krimissa, M., "Sorption isotherms: A review on physical bases, modeling and measurement". ***Applied Geochemistry***, Vol. 22, (2007), 249-275.
35. Li, Q., Su, H., Li, J., and Tan, T., "Application of surface molecular imprinting adsorbent in expanded bed for the adsorption of Ni2+ and adsorption model". ***Journal of Environmental Management***, Vol. 85, (2007), 900-907.
36. Kalavathy, H., Karthik, B., and Miranda, L.R., "Removal and recovery of Ni and Zn from aqueous solution using activated carbon from Hevea brasiliensis: Batch and column studies". ***Colloids and Surfaces B: Biointerfaces***, Vol. 78, (2010), 291-302.
37. Vijayaraghavan, K. and Prabu, D., "Potential of Sargassum wightii biomass for copper(II) removal from aqueous solutions: Application of different mathematical models to batch and continuous biosorption data***". Journal of Hazardous Materials***, Vol. 137, (2006), 558-564.
38. Senthilkumar, R., Vijayaraghavan, K., Thilakavathi, M., Iyer, P., and Velan, M., "Seaweeds for the remediation of wastewaters contaminated with zinc (II) ions". ***Journal of Hazardous Materials***, Vol. 136, (2006), 791-799.
39. Calero, M., Hernainz, F., Blazquez, G., Tenorio, G., and Martin-Lara, M., "Study of Cr(III) biosorption in a fixed-bed column". ***Journal of Hazardous Materials***, Vol. 171, (2009), 886-893.
40. Wu, J. and Yu, H.Q., "Biosorption of 2, 4-dichlorophenol by immobilized white-rot fungus Phanerochaete chrysosporium from aqueous solutions". ***Bioresource Technology***, Vol. 98, (2007), 253-259.
41. Song, J., Zou, W., Bian, Y., Su, F., and Han, R., "Adsorption characteristics of methylene blue by peanut husk in batch and column modes". ***Desalination***, Vol. 265, (2011), 119-125.
42. Zeinali, F., Ghoreyshi, A., and Najafpour, G., "Removal of toluen and dichloromethane from aqueous phase by Granular Activated Carbon (GAC)". ***Chemical Engineering Communications***, Vol. 199, (2012), 203-220.
43. Yan, G., Viraraghavan, T., and Chen, M., "A new model for heavy metal removal in a biosorption column". ***Adsorption Science & Technology***, Vol. 19, (2001), 25-43.
44. Turan, N.G., Mesci, B., and Ozgonenel, O., "Artificial neural network (ANN) approach for modeling Zn (II) adsorption from leachate using a new biosorbent". ***Chemical Engineering Journal***, Vol. 173, (2011), 98-105.
45. Zurada, J.M., "Introduction to artificial neural systems", West publishing companyx, St. Paul, Minnesota, (1992).
46. Widrow, B., Rumelhart, D.E., and Lehr, M.A., "Neural networks: Applications in industry, business and science". ***Communications of the ACM***, Vol. 37, (1994), 93-105.
47. Oguz, E. and Ersoy, M., "Removal of Cu2+ from aqueous solution by adsorption in a fixed bed column and Neural Network Modelling". ***Chemical Engineering Journal***, Vol. 164, (2010), 56-62.
48. Turan, N.G., Mesci, B., and Ozgonenel, O., "The use of artificial neural networks (ANN) for modeling of adsorption of Cu (II) from industrial leachate by pumice". ***Chemical Engineering Journal***, Vol. 171, (2011), 1091-1097.
49. Yetilmezsoy, K. and Demirel, S., "Artificial neural network (ANN) approach for modeling of Pb (II) adsorption from aqueous solution by Antep pistachio (Pistacia Vera L.) shells". ***Journal of Hazardous Materials***, Vol. 153, (2008), 1288-1300.
50. Özdemir, U., Özbay, B., Veli, S., and Zor, S., "Modeling adsorption of sodium dodecyl benzene sulfonate (SDBS) onto polyaniline (PANI) by using multi linear regression and artificial neural networks". ***Chemical Engineering Journal***, Vol. 178, (2011), 183-190.
51. Rajaee, T., Mirbagheri, S.A., Zounemat-Kermani, M., and Nourani, V., "Daily suspended sediment concentration simulation using ANN and neuro-fuzzy models". ***Science of the Total Environment***, Vol. 407, (2009), 4916-4927.
52. Khataee, A., Dehghan, G., Ebadi, A., Zarei, M., and Pourhassan, M., "Biological treatment of a dye solution by Macroalgae Chara sp.: Effect of operational parameters, intermediates identification and artificial neural network modeling". ***Bioresource Technology***, Vol. 101, (2010), 2252-2258.
53. Jha, S.K. and Madras, G., "Neural network modeling of adsorption equilibria of mixtures in supercritical fluids". ***Industrial & Engineering Chemistry Research***, Vol. 44, (2005), 7038-7041.
54. Tortum, A., The modeling of mode choices of intercity freight transportation with the artificial neural networks and integrated neuro-fuzzy system., Atatürk University: Turkish. (2003).
55. Haykin, S. and Network, N., "A comprehensive foundation". ***Neural Networks***, Vol. 2, (2004).
56. Pavia, D.L., Lampman, G.M., and Kriz, G.H., "Introduction to Spectroscopy", 3 ed, Brooks/Colex, Washington, (2001), 570.
57. Kannamba, B., Reddy, K.L., and AppaRao, B., "Removal of Cu (II) from aqueous solutions using chemically modified chitosan". ***Journal of Hazardous Materials***, Vol. 175, (2010), 939-948..

Adsorption of Fe(II) from Aqueous Phase by Chitosan: Application of Physical Models and Artificial Neural Network for Prediction of Breakthrough

H. Radnia[a], A. A. Ghoreyshi[a], H. Younesi[b], M. Masomi[a], K. Pirzadeh[a]

[a] *Chemical Engineering Department, Babol University of Technology, Babol, Iran*
[b] *Department of Environmental Science, Faculty of Natural Resources, Tarbiat Modares University, Noor, Iran*

P A P E R I N F O

Paper history:
Received 28 February 2013
Received in revised form 01 April 2013
Accepted 18 April 2013

Keywords:
Chitosan
Fe(II)
Adsorption
Breakthrough Curve
Artificial Neural Network

چکیده

در این مطالعه حذف یون آهن (II) از محیط آبی با استفاده از جاذب کیتوسان در سیستم‌های ناپیوسته و پیوسته مورد بررسی قرار گرفت. آزمایش‌های ناپیوسته در بازه غلظتی ۵۰-۱۰ mg/l و بازه دمایی ۴۰-۲۰ $^{\circ}C$ انجام پذیرفت. در آزمایش‌های ناپیوسته بیشترین ظرفیت جذب ۲۸mg/l و بیشترین راندمان حذف ۹۳٪ بوده است. داده‌های تعادلی جذب به خوبی با مدل لانگمیر-فرندلیچ برازش شد و ثوابت مدل بدست آمد. در مطالعه سیستم پیوسته، آزمایش‌ها در بستر ثابتی از جاذب کیتوسان با جریان رو به بالا و در دمای ثابت ۲۵$^{\circ}C$ انجام شد. در دبی‌های بالاتر، غلظت اولیه بالاتر فلز و ارتفاع کم‌تر بستر، منحنی‌های رخنه دارای شیب بیشتری بودند. منحنی‌های رخنه با مدل‌های فیزیکی توماس و یان، به همراه روش شبکه‌های عصبی مصنوعی مورد تحلیل قرار گرفتند. شبیه‌سازی دینامیکی رفتار سیستم با استفاده از شبکه عصبی مصنوعی (BP-ANN) انطباق بالاتری با داده‌های تجربی در مقایسه با مدل‌های فیزیکی نشان داد. آنالیز FTIR کیتوسان، قبل و بعد از فرایند جذب نشان داد که گروهای هیدروکسیل و آمینی، اصلی‌ترین گروه‌های عاملی شرکت کننده در جذب یون‌های آهن می‌باشند

doi: *10.5829/idosi.ije.2013.26.08b.06*